British Journal of Pharmacology

DOI:10.1111/bph.13386
www.brjpharmacol.org

RESEARCH PAPER

Trimetazidine prevents macrophage-mediated septic myocardial dysfunction via activation of the histone deacetylase sirtuin 1

Jing Chen[1], Jinsheng Lai[1], Lei Yang[1], Guoran Ruan[1], Sandip Chaugai[1], Qin Ning[2], Chen Chen[1] and Dao Wen Wang[1]

[1]Department of Internal Medicine and Gene Therapy Center, Tongji Hospital, Tongji Medical College, Huazhong University of Science and Technology, Wuhan, China, and [2]Department of Infectious Disease, Institute of Infectious Disease, Tongji Hospital of Tongji Medical College, Huazhong University of Science and Technology, Wuhan, China

Correspondence
Dao Wen Wang and Chen Chen, Department of Internal Medicine, Tongji Hospital, Tongji Medical College, Huazhong University of Science and Technology, 1095# Jiefang Ave., Wuhan 430030, China.
E-mail: dwwang@tjh.tjmu.edu.cn; chenchen@tjh.tjmu.edu.cn

Received
7 April 2015
Revised
13 October 2015
Accepted
18 October 2015

BACKGROUND AND PURPOSE

Sepsis is a systemic inflammatory response accompanied by excessive production of inflammatory cytokines and cardiovascular dysfunction. Importantly, macrophage-derived pro-inflammatory agents play a key role in cardiovascular impairment in sepsis. Here we have investigated the effects of trimetazidine (TMZ) on pro-inflammatory responses of macrophages in endotoxin-induced myocardial dysfunction.

EXPERIMENTAL APPROACH

Mice pretreated with TMZ were injected i.p. with LPS and cardiac function evaluated. Levels of macrophage infiltration, macrophage inflammatory response and cardiomyocyte apoptosis were measured using immunohistochemical staining, ELISA, real-time RT-PCR, Western blot, TUNEL and flow cytometry assays.

KEY RESULTS

Pretreatment with TMZ prevented LPS-induced myocardial dysfunction and apoptosis. TMZ also lowered levels of pro-inflammatory cytokines in serum and cardiac tissue and myocardial macrophage infiltration. Bone marrow transplantation indicated that TMZ alleviated LPS-induced myocardial dysfunction via decreasing macrophage infiltration. TMZ reduced expression of pro-inflammatory cytokines in LPS-stimulated cardiac and peritoneal macrophages. Co-culture of TMZ-pretreated macrophages with cardiomyocytes and conditioned media from TMZ-pretreated macrophages both decreased LPS-induced cardiomyocyte apoptosis. The anti-apoptosis effects of TMZ resulted from decrease of pro-inflammatory cytokines, partly due to normalizing the sirtuin 1 (Sirt1)/AMP-activated protein kinase (AMPK)/Nrf2/haem oxygenase-1 and Sirt1/PPARα pathways in macrophages. Cytokine secretion was also regulated by ROS, which were attenuated by TMZ via activation of Sirt1, AMPK and PPARα.

CONCLUSIONS AND IMPLICATIONS

TMZ protected against LPS-induced myocardial dysfunction and apoptosis, accompanied by inhibition of macrophage pro-inflammatory responses. Our studies suggest that TMZ might represent a novel therapeutic agent to prevent and treat sepsis-induced myocardial dysfunction.

Abbreviations

AMPK, AMP-activated protein kinase; DHE, dihydroethidium; H&E, haematoxylin–eosin; HO-1, haem oxygenase-1; i.g, intragastric; NAC, N-acetylcysteine; NAM, nicotinamide; Nrf2, nuclear factor erythroid 2-related factor 2; ROS, reactive oxygen species; Sirt1, sirtuin 1; TMZ, trimetazidine

Tables of Links

TARGETS
Enzymes[a]
Sirt1, sirtuin 1
AMPK, AMP kinase
HO-1, haem oxygenase 1
Nuclear hormone receptors[b]
PPARα

LIGANDS
CCL2
Compound C, dorsomorphin
GW6471
IL-1β
IL-6
TNFα

These Tables list key protein targets and ligands in this article which are hyperlinked to corresponding entries in http://www.guidetopharmacology.org, the common portal for data from the IUPHAR/BPS Guide to PHARMACOLOGY (Pawson *et al.*, 2014) and are permanently archived in the Concise Guide to PHARMACOLOGY 2013/14 ([a b]Alexander *et al.*, 2013a, b).

Introduction

Sepsis is defined as a systemic inflammatory response to the presence of microbial pathogens. Bacterial endotoxin LPS is considered to be the principal cause of multi-organ failure in sepsis, including myocardial depression (Opal *et al.*, 1999). At cellular level, sepsis is provoked by an overwhelming inflammatory response initiated by the innate immune system. In particular, activated macrophages trigger a potentially fatal immune reaction via excessive production of pro-inflammatory cytokines and reactive oxygen (Brown and Jones, 2004). This overwhelming inflammatory reaction can produce reversible or irreversible damage to cardiomyocytes, such as impairment of contractile efficiency and cell apoptosis. Apoptosis is a major cause for sepsis-induced heart dysfunction (McDonald *et al.*, 2000; Dispersyn and Borgers, 2001; Fauvel *et al.*, 2001). Therefore, controlling the excessive inflammatory reactions in macrophages may become an effective therapeutic strategy against sepsis-induced cardiac dysfunction.

LPS-induced macrophage inflammatory response is mediated through the toll-like receptors (TLR), leading to the release of pro-inflammatory cytokines (Ward, 2009). Induction of pro-inflammatory cytokines is mediated via the activation of many factors in macrophages. Sirtuin 1 (Sirt1), a NAD^+-dependent histone deacetylase, has been implicated in the regulation of a variety of physiopathological processes, such as inflammation, metabolism, apoptosis and ageing (Michan and Sinclair, 2007). Sirt1 was also shown to inhibit free radical-mediated oxidative injuries via decreasing NADPH oxidase activation (Kitada *et al.*, 2011). It has been shown that Sirt1 deacetylates LKB1 and secondarily affects the activity of AMP-activated protein kinase (AMPK) (Lan *et al.*, 2008). As a sensor of intracellular energy status, AMPK is an attractive target for inflammation control. Furthermore, as an antioxidative pathway, the transcription factor Nrf2 has been identified as the downstream partner of AMPK in inflammation suppression (Mo *et al.*, 2014).

PPARs are ligand-activated transcription factors and have been shown to regulate inflammation through the NF-κB pathway (Daynes and Jones, 2002). Recently, it has been reported that Sirt1 acted with PPARα to protect cardiomyocytes from inflammation (Planavila *et al.*, 2011).

Trimetazidine (TMZ), a piperazine derivative used as an antianginal agent, selectively inhibits long-chain 3-ketoacyl coenzyme A thiolase activity. TMZ may affect myocardial substrate consumption by inhibiting oxidative phosphorylation and shifting energy production from free fatty acids (FFA) to glucose oxidation (Onay-Besikci and Ozkan, 2008). TMZ also has been reported to have a potential benefit in inflammation (Zhou *et al.*, 2012).

Here we have confirmed the effect of TMZ in endotoxin-induced myocardial dysfunction and have explored the possible mechanisms, in terms of the pro-inflammatory responses of macrophages

Methods

Animals

All animal care and experimental protocols complied with the National Institutes of Health Guidelines for the Care and Use of Laboratory Animals and were approved by The Academy of Sciences of China. These studies comply with the recommendations on experimental design and analysis in pharmacology (Curtis *et al.*, 2015). The animal studies follow the ARRIVE guidelines (McGrath, McLachlan and Zeller, 2015; McGrath and Lilley, 2015) and complied with the principles of replacement, refinement and reduction (the 3Rs).

Ten-week-old male C57BL/6 mice (Institutional Animal Research Committee of Tongji Medical College, Wuhan, China) were used in this study, and the weight of the animals was around 25 g. All these mice were raised in the specific pathogen free (SPF) animal centre of Tongji Hospital, Tongji Medical College, Huazhong University of Science and Technology (Wuhan, China). The mice were maintained at a room temperature of 23 ± 1°C and 55 ± 5% humidity with a 12 h light/dark cycle and access to food and water *ad libitum*. The food was sterilized with high pressure. The drinking water was supplied by a reverse osmosis water treatment system and sterilized by filtration and ozone. The water bottles were changed every week. All the mice were housed in polycarbonate,ventilated cages and received irradiated corncob

bedding. The cages were changed every 2 weeks, while the bedding was changed weekly. There were two mice in each cage.

Experimental procedures

Group sizes. To evaluate the effects of TMZ pretreatment before LPS stimulation, the mice were divided into four groups, saline control (n = 8), TMZ (n = 8), LPS (n = 8) and TMZ plus LPS (n = 8) group. To evaluate the therapeutic effects of TMZ treatment after LPS stimulation, mice were divided randomly into four groups, saline control (n = 8), TMZ (n = 8), LPS (n = 8) and TMZ plus LPS (n = 8). To evaluate the effects of TMZ on mortality of LPS-induced sepsis myocardial dysfunction, 80 mice were randomly divided into four groups, saline control (n = 20), TMZ (n = 20), LPS (n = 20) and TMZ plus LPS (n = 20). For the bone marrow implantation, there were eight mice in each group.

Randomization. We used the random number table to perform the randomization. First, all mice were weighed and ordered by their weight from light to heavy. Then we chose a number from the random number table randomly and allocated that number to the lightest mouse. As four groups were needed in total, we divided the number by four. If this number was divisible by 4, the mouse would be placed in the first group, if not divisible by 4 but with remainder 1, the mouse would be placed in the second group. The third and the fourth groups were made up similarly. After the lightest mouse was grouped, the number on the right of prior in the random number table was given to the second mouse, and similar methods were taken to group the mouse until all mice were grouped.

Blinding. All the data were collected and analysed by two observers who were not aware of the group assignment or treatment of animals.

Validity of animal species or model selection. In the present study, LPS injected i.p. in a dose of 15 mg · kg^{-1} was used to induce the septic cardiac dysfunction, because it was the classical endotoxin as an inducer for sepsis. Besides, mice were chosen in the study not only because of their high homology with human but also the sensitivity to the rapid progress of the sepsis.

General procedures. All surgery was performed under sodium pentobarbital anaesthesia, and all efforts were made to minimize suffering. The operations that could cause pain and distress were performed in another room without other animals being present. Mice were anaesthetized with i.p. injections of xylazine (5 mg · kg^{-1}) and ketamine (80 mg · kg^{-1}) mixture; they were placed in a supine position before they were killed. At the end of the experiment, animals were killed by CO_2 inhalation, which was performed in a professional and compassionate manner by skilled personnel.

Morphological analysis. For histopathological examination, the mice in each group were killed at 6 h after LPS injection. Heart tissues were fixed in 10% formalin, embedded in paraffin, sectioned and then stained with haematoxylin–eosin (H&E) for morphological analysis. Slides were imaged using a Nikon microscope (Nikon, Tokyo, Japan). To determine cardiomyocyte cross-sectional areas, H&E slides were analysed by outlining round to cuboidal-shaped nucleated myocytes.

Echocardiography. Left ventricular dynamics was assessed by echocardiography as described previously (Turdi *et al.*, 2012). Left ventricular end-diastolic dimension (LVEDD) was measured at the time of the apparent maximal left ventricular diastolic dimension, and left ventricular end-systolic dimension (LVESD) was measured at the time of the most anterior systolic excursion of the posterior wall. Left ventricular ejection fraction (LVEF) was calculated using the following formula: LVEF (%) = 100 × (LVEDD^3 − LVESD^3)/LVEDD^3.

Cell culture and sorting. Primary peritoneal macrophages from male C57BL/6 mice (10 weeks of age, purchased from The Institutional Animal Research Committee of Tongji Medical College, Wuhan, China) were isolated 3 days after i.p. injection of thioglycollate and cultured in RPMI-1640 medium (Life Technologies, Cergy-Pontoise, France) supplemented with 10% FBS and maintained in a humidified 5% CO_2 atmosphere at 37°C and used for experiments.

Neonatal myocardial cells were isolated from collagenase digested hearts as described previously (Minhas *et al.*, 2005) and used in macrophage–cardiomyocyte co-culture and conditional medium culture models. To evaluate the apoptosis of cardiomyocytes, cells were washed twice with PBS and stained with Annexin V-FITC and propidium iodide in 1× Annexin binding buffer for 30 min. Cells were then washed twice with staining buffer and subjected to FACScan (BD Biosciences, Franklin Lakes, NJ, USA). Data were analysed by CellQuest software (BD Biosciences) or FlowJo Version 7.6.1.

Single-cell suspensions were obtained from mouse heart. Briefly, anaesthetized mice were perfused through the left ventricle (LV) with 25 mL of ice-cold PBS. Heart tissues were excised and minced with fine scissors prior to digestion in 1 mg · mL^{-1} Collagenase/Dispase (Roche) for 1 h at 37°C under agitation. Tissues were triturated, and cells were filtered through a 40 μm nylon mesh (BD Falcon), then washed and centrifuged (8 min, 300 g, 4°C). Erythrocytes were removed using RBC Lysis Buffer (eBioscience, San Diego, CA, USA). Single-cell suspensions from heart were stained at 4°C in PBS with FACS buffer for 1 h. Fluorochrome-antibodies specific to CD45-APC, CD11b-FITC, Ly6C-PerCP-Cy5.5 and mouse F4/80-PE were used (eBioscience, San Diego, CA, USA). Cells were then washed twice with staining buffer and subjected to FACScan. Data were analysed by FlowJo Version 7.6.1.

Cardiac CD45$^+$CD11b$^+$F4/80$^+$ macrophages were sorted on AriaII instrumentation (BD Bioscience). The purity was almost >95%. The sorted cells were collected to prepare RNA samples immediately.

Bone marrow transplantation. We performed bone marrow transplantation in wild type (WT) C57/BL6 mice as described earlier (Zhang *et al.*, 2004). Briefly, 10-week-old WT C57/BL6 mice were pretreated with TMZ (20 mg · kg^{-1} in saline solution at 6 mg · mL^{-1}, intragastric (i.g.), t.i.d., for 3 days) or equal amount of solvent (saline solution) as control, and then the mice received 950 rads of γ-irradiation and were treated with the antibiotic, Bayril. The next day, fresh bone marrow cells were isolated from a separate cohort of WT C57/BL6 control mice and non-irradiated TMZ pretreated mice, respectively, and were injected into irradiated mice (6 × 10^6 cells) in 200 μL volume through the tail vein. Twelve hours after bone marrow transplantation, the mice were given LPS

(i.p.; 15 mg · kg^{-1}), and all mice survived the LPS challenge. Six hours after LPS administration, hearts were collected for immunohistochemistry, F4/80 staining and other tests.

Immunohistochemical staining. Mice were pretreated with TMZ (20 mg · kg^{-1}, i.g., t.i.d.) or saline for 3 days, and then injected with 15 mg · kg^{-1} LPS or saline. After LPS stimulation for 6 h, the mice in each group were killed for heart sample collection, which were used in the subsequent immunostaining. The infiltration of macrophages was assessed using immunohistochemical assays. Sections (2 μm) were dewaxed, incubated with 3% H_2O_2, blocking serum and thereafter with a polyclonal antibody against F4/80 (Santa Cruz Biotechnologies, CA, USA) at 1:100 dilution. Slides were imaged using a Nikon microscope (Nikon). Quantification of the immunohistochemistry results was carried out with IMAGE PRO PLUS software.

Evaluation of apoptosis by TUNEL. Mice were pretreated with TMZ (20 mg · kg^{-1}, i.g.,t.i.d.) or saline for 3 days, and then injected with 15 mg · kg^{-1} LPS or saline. TUNEL assay was performed in heart tissue sections, which were collected 6 h after LPS stimulation using the FragEL DNA Fragmentation Detection Kit (Calbiochem, Billerica, MA, USA) according to the manufacturer' protocols. Slides were imaged using a Nikon microscope (Nikon). Results are expressed as number of TUNEL-positive cells/total cells × 100%.

Transfection with siRNA. Primary macrophages were plated at a density of 5 × 10^6 cells per well in six-well plates approximately 20 h prior to transfection. The macrophages were transfected with 100 nM siRNA for Sirt1 using lipofectamine 2000 (Invitrogen, Carlsbad, CA, USA), according to the manufacturer's instruction. After 24 h, the cells were treated with TMZ for 1 h and then LPS stimulation. After 6 h incubation, cells were prepared for DHE staining, RT-PCR or Western blot.

Macrophage–cardiomyocyte co-culture model. Peritoneal macrophages were pretreated with TMZ (20 μM) or inflammatory cytokines antibodies for 1 h and then stimulated with/without LPS (5 μg · mL^{-1}) for 6 h, washed and seeded onto transwell inserts above neonatal myocardial cells for 24 h of co-culture. At the end of co-culture, myocardial cells were used for apoptosis assay by flow cytometry.

Indirect co-culture model. Peritoneal macrophages were pretreated with the specific inhibitors, nicotinamide (NAM), Compound C or GW6471, and TMZ (20 μM) for 1 h and then stimulated with LPS (5 μg · mL^{-1}) for 6 h and washed, and conditioned medium (CM) from macrophages were collected. The cytokines in CM from synchronous experiment were measured with ELISA kits from R&D (R&D Systems, Inc., Minneapolis, MN, USA). Neonatal myocardial cells were incubated with CM for 18 h. At the end of CM co-culture, myocardial cells were assayed for apoptosis by flow cytometry.

Detection of ROS production. To evaluate production of ROS (in particular, O_2^-), primary peritoneal macrophages were pretreated with related inhibitors and incubated with freshly prepared TMZ alone (20 μM) or N-acetylcysteine (NAC) (5 mM) or TMZ with LPS (5 μg · mL^{-1}) for 6 h. Cells were washed twice with warm PBS (37°C) and further incubated for 1 h with DHE (2 mmol · L^{-1}; Molecular Probes, D-1168) in a CO_2 humidified incubator at 37°C, as previously described (Vivot *et al.*, 2014). Fluorescent images were captured after 1 h incubation with DHE using fluorescence microscopy (Nikon). All values for each treatment group was recorded as mean fluorescence intensity.

Quantitative real-time PCR. Total RNA was extracted, using TRIzol Reagent (Invitrogen), from cardiac macrophages, peritoneal macrophages and heart tissues, collected 6 h after LPS stimulation. cDNAs were reverse-transcribed from 1 μg RNA with reverse transcription kit (Thermo Electron, Waltham, MA, USA) and used as templates in quantitative

Table 1

Primers used for quantitative RT-PCR

Gene	Forward primer	Reverse primer
Mouse TNF-α	5'CCCTCACACTCAGATCATCTTCT3'	5'GCTACGACGTGGGCTACAG3'
Mouse CCL2	5'CGCTCAGCCAGATGCAATTA3'	5'GCCTCTGCATGGAGATCTTCTT3'
Mouse IL-1β	5'GCAACTGTTCCTGAACTCAACT3'	5'ATCTTTTGGGGTCCGTCAACT3'
Mouse IL-6	5'CTGCAAGAGACTTCCATCCAG3'	5'AGTGGTATAGACAGGTCTGTTGG3'
Mouse CPT-1	5'CGTTCACGCCATGATCATGT3'	5'AGAGCCAGACCTTGAAGAAG3'
Mouse CD36	5'GGAGCCATCTTTGAGCCTTCA3'	5'GAACCAAACTGAGGAATGGATCT3'
Mouse FABP3	5'ACCTGGAAGCTAGTGGACAG3'	5'TGATGGTAGTAGGCTTGGTCAT3'
Mouse Glut4	5'TACGGTCTTCACGTTGGTCT3'	5'CACGATGGAGACATAGCTCA3'
Mouse PDK4	5'AGGGAGGTCGAGCTGTTCTC3'	5'GGAGTGTTCACTAAGCGGTCA3'
Mouse GAPDH	5'CAAAATGGTGAAGGTCGGTGTG3'	5'TGATGTTAGTGGGGTCTCGCTC3'
Mouse 18S RNA	5'GGAAGGGCACCACCAGGAGT3'	5'TGCAGCCCCGGACATCTAAG3'

real-time PCR using SYBR Green Super mix kit (Thermo Electron). The sequences of primers used for PCR amplification are shown in Table 1. GAPDH served as internal normalization control.

Western blot assays. Whole cell lysates were prepared by directly denaturing macrophage pellets and homogenized heart tissues, collected 6 h after LPS stimulation, in SDS loading buffer and immediately boiled for 5 min. Nuclear and cytoplasmic protein fragmentation was performed according to the manufacturer's instructions (Boster, Wuhan, China). Western blot assays were performed as described previously (Hu *et al*., 2008). The following antibodies were applied: gp91, p47, PPARα, Nrf2, p-IκBα, IκBα, p65 and GAPDH were from Santa Cruz Biotechnologies. Sirt1 was from Beyotime (Beyotime, Shanghai, China). p-AMPK and AMPK were from Cell Signaling Technology (CST, Danvers, MA, USA). Haem oxygenase-1 (HO-1) was from ABclonal (ABclonal Biotechnology Co., Ltd. Wuhan, China). LaminB (Boster) was regarded as internal control. Bands were quantified by densitometry using QUANTITY ONE software (Bio-Rad, Hercules, CA, USA).

Data analysis. All data are shown as means ± SEM. The following data were normalized: cardiomyocytes cross-sectional area, measurement of Millar catheter, dihydroethidium (DHE) fluorescence intensity, quantitative analysis of Western blotting and the expression of mRNA. Moreover, for the data sets of Western blotting and the expression of mRNA, all the data were adjusted by the values of internal standard (such as GAPDH or Lamin B). Firstly, we calculated the control mean and then expressed all the individual control values and all the individual test values as fold of control mean and conducted appropriate statistical analyses on these normalized values (Curtis *et al*., 2015). Meanwhile, the Y axis was labelled as fold of control *mean*. There was no data transformation in our experiments.

All analyses were performed using PASW Statistics 18 software (SPSS Inc., Chicago, IL, USA). Student's unpaired *t*-test was used for comparing the data from two groups, whereas one-way ANOVA with the Bonferroni *post hoc* test was used for comparison among more than two groups. Survival rates were analysed by the Kaplan–Meier log-rank test and Pearson's correlation coefficient was used to measure the linear relationship between two variables. Significance was established at $P < 0.05$.

Materials. The compounds used in these experiments were supplied as follows: TMZ by Servier (Orléans, France); NAC and NAM by Beyotime (Shanghai, China); Compound C by Selleck Chemicals (Houston, TX); GW6471 by Sigma (St. Louis, MO).

Results

TMZ ameliorated myocardial dysfunction, apoptosis and improved survival in LPS-induced mice

To investigate whether TMZ exerted a protective effect on sepsis-induced cardiac dysfunction, 10-week-old male C57BL/6 mice were pretreated with TMZ for 3 consecutive days and then challenged with LPS by i.p. injection for 6 h. H&E staining of the myocardium obtained at 6 h after LPS injection showed mild oedema throughout the myocardium, as shown by the cardiomyocyte cross-sectional area. The oedema was attenuated in mice treated with LPS plus TMZ (Figure 1). Meanwhile, the cardiomyocyte apoptosis induced by LPS was also attenuated by TMZ pretreatment (Figure 1).

Moreover, myocardial function was impaired in LPS-challenged mice, as shown by decreased ejection fraction, fractional shortening (Figure 1) and LV dp/dt (Figure 1), increased left ventricular internal diameter (Figure 1) and LVEDP (Figure 1). Interestingly, TMZ pretreatment attenuated the development of myocardial dysfunction. Furthermore, to evaluate the therapeutic effects of TMZ after LPS stimulation, mice were first injected with LPS for 6 h and then treated with TMZ for 24 h. This TMZ post-treatment, after LPS challenge, also improved cardiac function (Figure 1). Moreover, median arterial pressure (MAP) measurements and survival analysis indicated TMZ decreased the hypotension and improved survival rate in LPS-challenged mice (Figure 1). These data suggested that TMZ treatment attenuated LPS compromised myocardial dysfunction and apoptosis.

TMZ pretreatment-reduced systemic and local pro-inflammatory responses and myocardial infiltration by macrophages, in LPS-treated mice

Mice were pretreated with TMZ or saline for 3 days and then injected with LPS or saline for 6 h. After LPS stimulation, the levels of the pro-inflammatory cytokines, TNF-α, CCL2, IL-1β and IL-6, in plasma and heart tissues were both significantly increased. Pretreatment with TMZ significantly attenuated these inflammatory responses (Figure 2). In addition, F4/80 staining revealed that the number of macrophages within myocardial tissue was increased in LPS-treated animals, but similar macrophage infiltration was not present in TMZ-pretreated mice (Figure 2).

TMZ-pretreated bone marrow ameliorated the myocardial dysfunction and myocardial macrophage accumulation induced by LPS

To further assess whether pretreatment with TMZ of bone marrow or myocardium was responsible for reducing macrophage infiltration, we performed reciprocal bone marrow transplantation between TMZ-pretreated mice and WT mice. After recovery from transplantation, mice were injected i.p. with LPS. Quantification of macrophages by F4/80 staining showed that bone marrow from TMZ-pretreated mice decreased myocardial macrophage infiltration in both WT and TMZ-pretreated recipient mice, accompanied with normalized myocardial structure (Figure 3). Moreover, assessment of cardiac function showed that bone marrow from TMZ-pretreated mice increased ejection fraction, fractional shortening, LVESP, LV dp/dt and decreased left ventricular internal diameter and LVEDP in TMZ > WT and TMZ > TMZ mice (Figure 3). These data suggested that the improvement of cardiac function in TMZ > WT and TMZ > TMZ mice was associated with reduced infiltration of macrophages. Moreover, the correlation analysis showed that there was a significant negative correlation between the numbers of

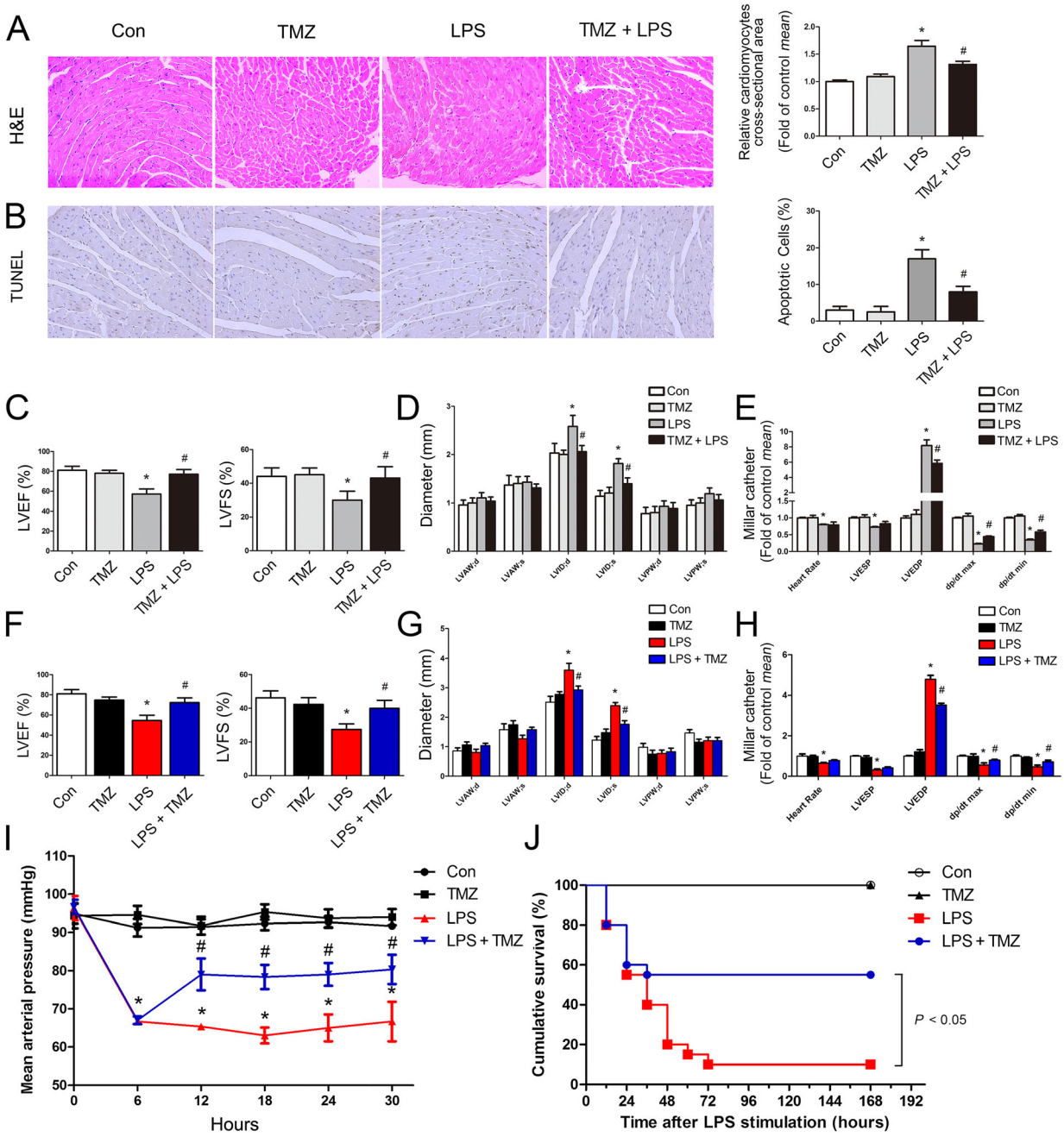

Figure 1

TMZ ameliorated myocardial dysfunction and apoptosis in LPS-induced mice. Mice were pretreated with TMZ (20 mg · kg^{-1}, i.g., t.i.d.) for 3 days and then injected with 15 mg · kg^{-1} LPS (n = 8 in each group). (A) Left, representative images of left ventricular myocardium H&E staining; right, quantification of the size of cardiomyocytes by measurement of cross-sectional area. (B) Left, representative images of TUNEL staining of left ventricular myocardium; right, quantitative analysis of TUNEL-positive cells (original magnification was 200×). Data were expressed as percentage of TUNEL-positive nuclei/total nuclei. (C–D) LVEF, LVFS, LVAW, LVID and LVPW were measured by two-dimensional echocardiography. (E) Heart rate, LVESP, LVEDP, dp/dt max and dp/dt min were evaluated by cardiac catheterization. Mice were first injected with LPS (15 mg · kg^{-1}, i.p.) for 6 h, then TMZ (20 mg · kg^{-1}, i.g., t.i.d.) were given for 1 day (n = 8 in each group). (F–G) LVEF, LVFS, LVAW, LVID and LVPW were measured by two-dimensional echocardiography. (H) Heart rate, LVESP, LVEDP and LV dp/dt from each group mice were evaluated by cardiac catheterization. (I) Average MAP was recorded by a tail-cuff method. (J) C57BL/6 mice were first injected with LPS (15 mg · kg^{-1}, i.p.) for 6 h, then TMZ (20 mg · kg^{-1}, i.g., t.i.d.) were given for 3 days (n = 20 in each group). Kaplan–Meier survival plots for each group treated as earlier. The groups were designated as follows: Con, saline group; LPS, LPS-injected group; TMZ, TMZ only group; TMZ + LPS, mice were pretreated with TMZ then injected with LPS; LPS + TMZ, mice were injected with LPS then treated with TMZ. *$P < 0.05$ vs. control; $^{\#}P < 0.05$ vs. LPS-treated group. Data in (J) were analysed by the Kaplan–Meier log-rank test. Other data were analysed by one-way ANOVA. LVAW, left ventricular anterior wall; LVID, left ventricular internal diameter; LVPW, left ventricular posterior wall; LVEDP, left ventricular end diastolic pressure; LVFS, left ventricular fractional shortening; LVESP, left ventricular end systolic pressure.

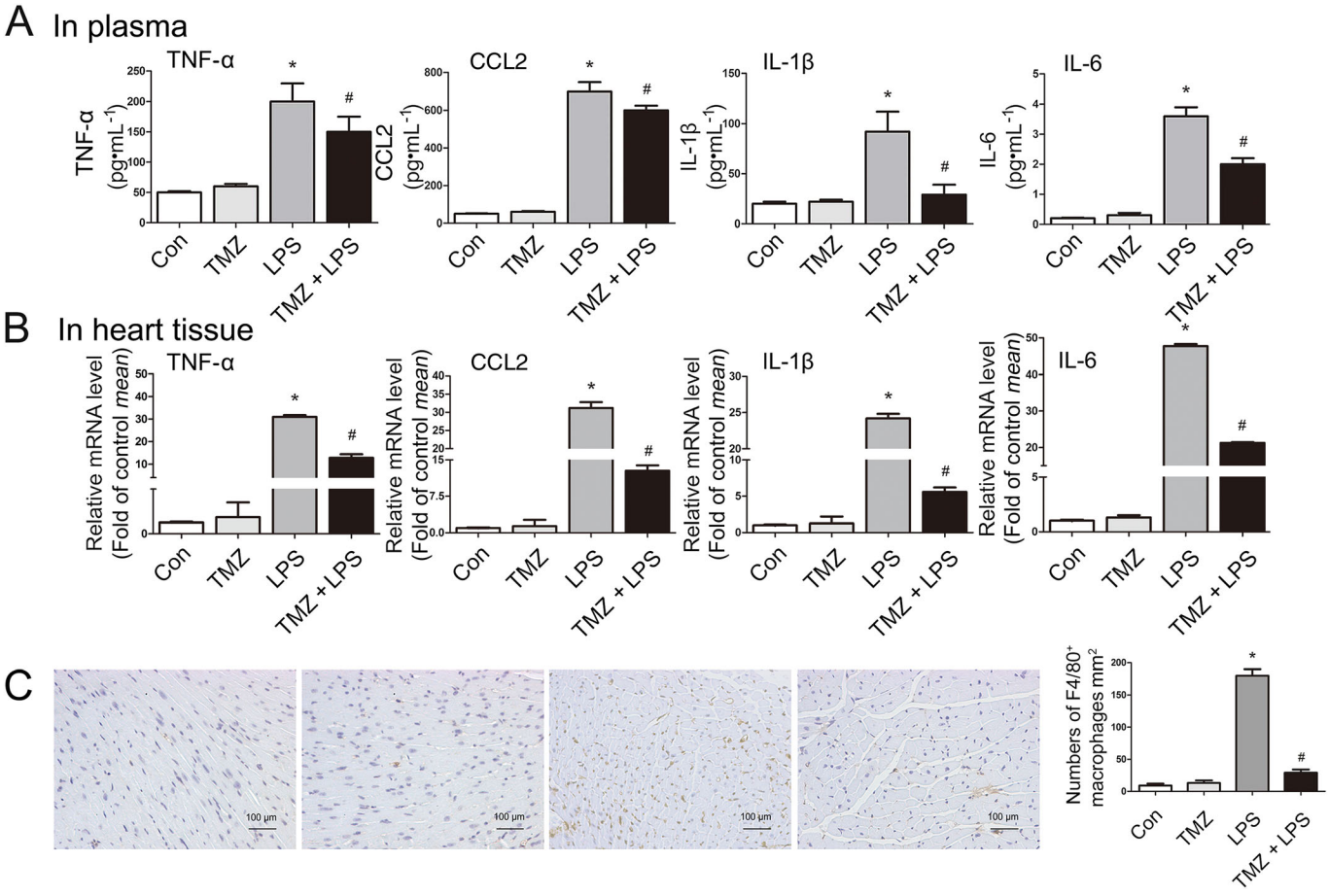

Figure 2

TMZ pretreatment reduced systemic and local pro-inflammatory response and myocardial macrophage infiltration in LPS-treated mice. (A) Mice were pretreated with TMZ (20 mg · kg^{-1}, i.g., t.i.d.) for 3 days and then injected with 15 mg · kg^{-1} LPS (n = 8 in each group). The plasma of mice was collected, and protein levels of pro-inflammatory cytokines (TNF-α, CCL2, IL-1β and IL-6) were determined by ELISA assay. (B) The heart tissues were collected to prepare for RNA samples. RT-PCR was performed to detect cardiac pro-inflammatory cytokines levels. (C) Left, F4/80 staining of left ventricular myocardium was presented from C57BL/6 mice. Original magnification was 200× and scales = 100 μm. Right, quantitative analysis of F4/80-positive cells in 1 mm^2 of area. The groups were designated as follows: Con, saline group; LPS, LPS-injected group; TMZ, TMZ only group; TMZ + LPS, mice were pretreated with TMZ then injected with LPS. Data shown are means ± SEM of three separate experiments. *$P < 0.05$ vs. control; $^{\#}P < 0.05$ vs. LPS-treated group; one-way ANOVA.

myocardial macrophages in recipient mice and cardiac function, evaluated by LVEF, LVFS, dp/dt max and dp/dt min (Supporting Information Fig. S1). Furthermore, flow cytometry also revealed that bone marrow from TMZ-pretreated mice decreased the number of CD11b$^+$F4/80$^+$ macrophages in TMZ > WT and TMZ > TMZ mice (Figure 3). The decreased accumulation of macrophages in the myocardium of TMZ > WT and TMZ > TMZ mice was paralleled by decreased numbers of their precursors, CD11b$^+$Ly6C$^+$ monocytes, indicating that TMZ affected the recruitment of monocytes (Figure 3G and H).

TMZ treatment attenuated the cardiomyocyte apoptosis mediated by the pro-inflammatory response of macrophages

To determine the behaviour of macrophages present within the heart, we sorted by FACS, the CD45$^+$CD11b$^+$F4/80$^+$ cardiac macrophages from mice injected with LPS, with or without pretreatment with TMZ. The gating strategy is shown in Figure 4. Sorted cardiac macrophages were collected to prepare RNA samples and then used for RT-PCR analysis. The results showed that, compared with LPS, TMZ pretreatment reduced the expression of pro-inflammatory cytokines (TNF-α, CCL2, IL-1β and IL-6) in CD45$^+$CD11b$^+$F4/80$^+$ cardiac macrophages in LPS-injected mice (Figure 4). The result was consistent with data obtained in peritoneal macrophages (Figure 4). These results suggested that the general effects of LPS and TMZ on cardiac macrophages and peritoneal macrophages were the same. Thus, the peritoneal macrophages were used in the following experiments. The results of co-cultures of LPS-activated peritoneal macrophages with neonatal myocardial cells revealed that LPS-activated macrophages markedly induced apoptosis of neonatal myocardial cells, but TMZ pretreatment prevented this apoptosis (Figure 4). We next determined the roles of the pro-inflammatory cytokines by blocking them with neutralizing

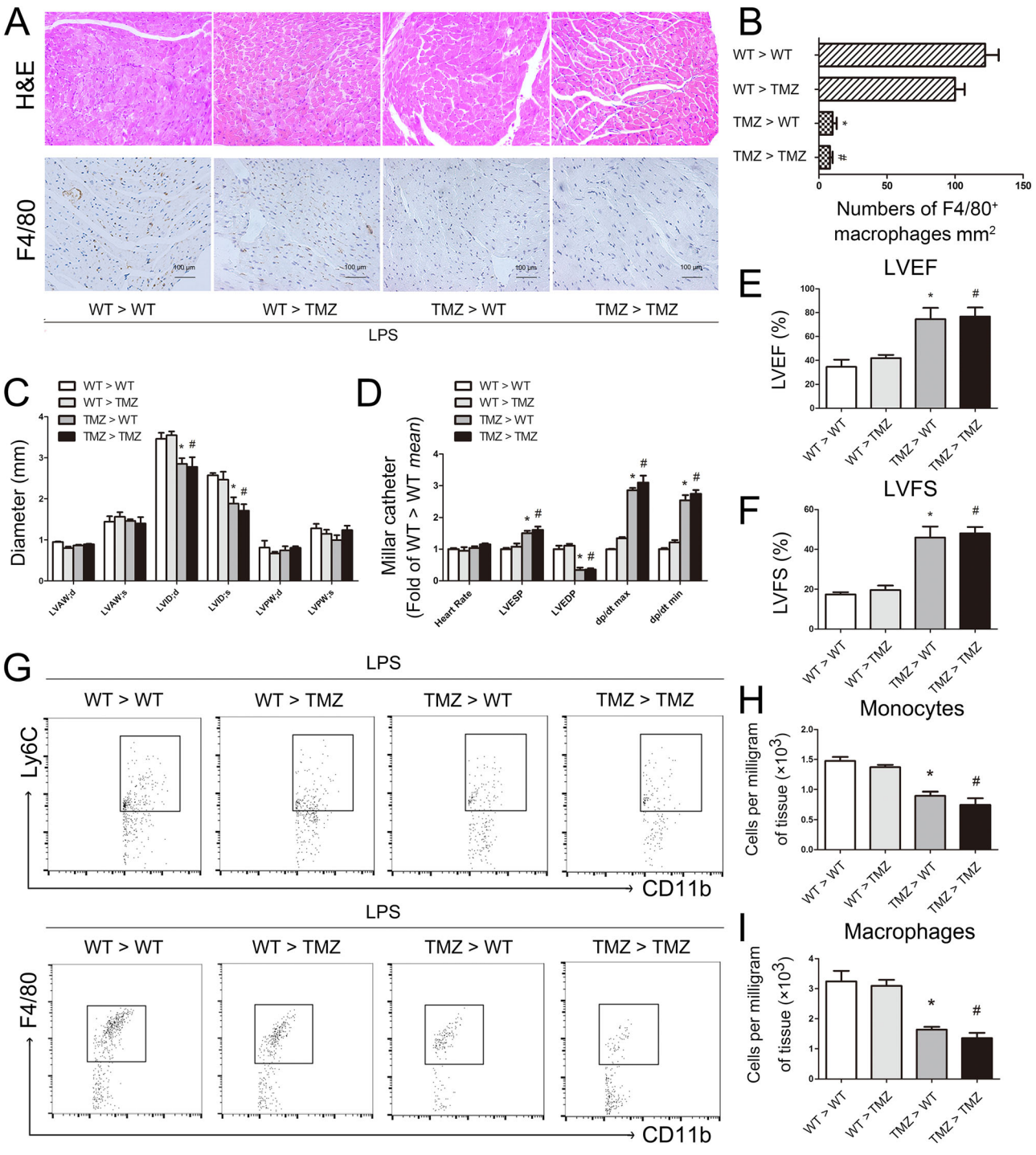

Figure 3

TMZ-pretreated bone marrow-ameliorated LPS-induced myocardial dysfunction and myocardial macrophage accumulation. (A) Irradiated TMZ pretreated (20 mg · kg^{-1}, i.g., t.i.d., for 3 days) and WT received either WT or TMZ-pretreated bone marrow subjected to LPS challenge (15 mg · kg^{-1}). Top, H&E staining showed myocardial structures after bone marrow transplantation; original magnification was 200×. Bottom, F4/80-stained macrophages in the myocardium were imaged at 200× and scales = 100 μm. (B) Quantitative analysis of F4/80-positive cells in 1 mm^2 of area. (C) LVAW, LVID and LVPW were measured in the two-dimensional echocardiography. (D) Heart rate, LVESP, LVEDP, dp/dt max and dp/dt min were evaluated by cardiac catheterization. (E–F) LVEF and LVFS were measured in the two-dimensional echocardiography. (G) Dot plots showed CD11b$^+$Ly6C$^+$ monocytes and CD11b$^+$F4/80$^+$ macrophages in heart tissues from the recipient mice. (H) Numbers of CD11b$^+$Ly6C$^+$ monocytes in different groups per mg of heart tissue. (I) Numbers of CD11b$^+$F4/80$^+$ macrophages in different groups per mg of heart tissue. Data shown are means ± SEM of three separate experiments. *$P < 0.05$ vs. WT > WT mice; $^{\#}P < 0.05$ vs. WT > TMZ mice; one-way ANOVA. LVAW, left ventricular anterior wall; LVID, left ventricular internal diameter; LVPW, left ventricular posterior wall; LVEDP, left ventricular end diastolic pressure; LVFS, left ventricular fractional shortening; LVESP, left ventricular end systolic pressure.

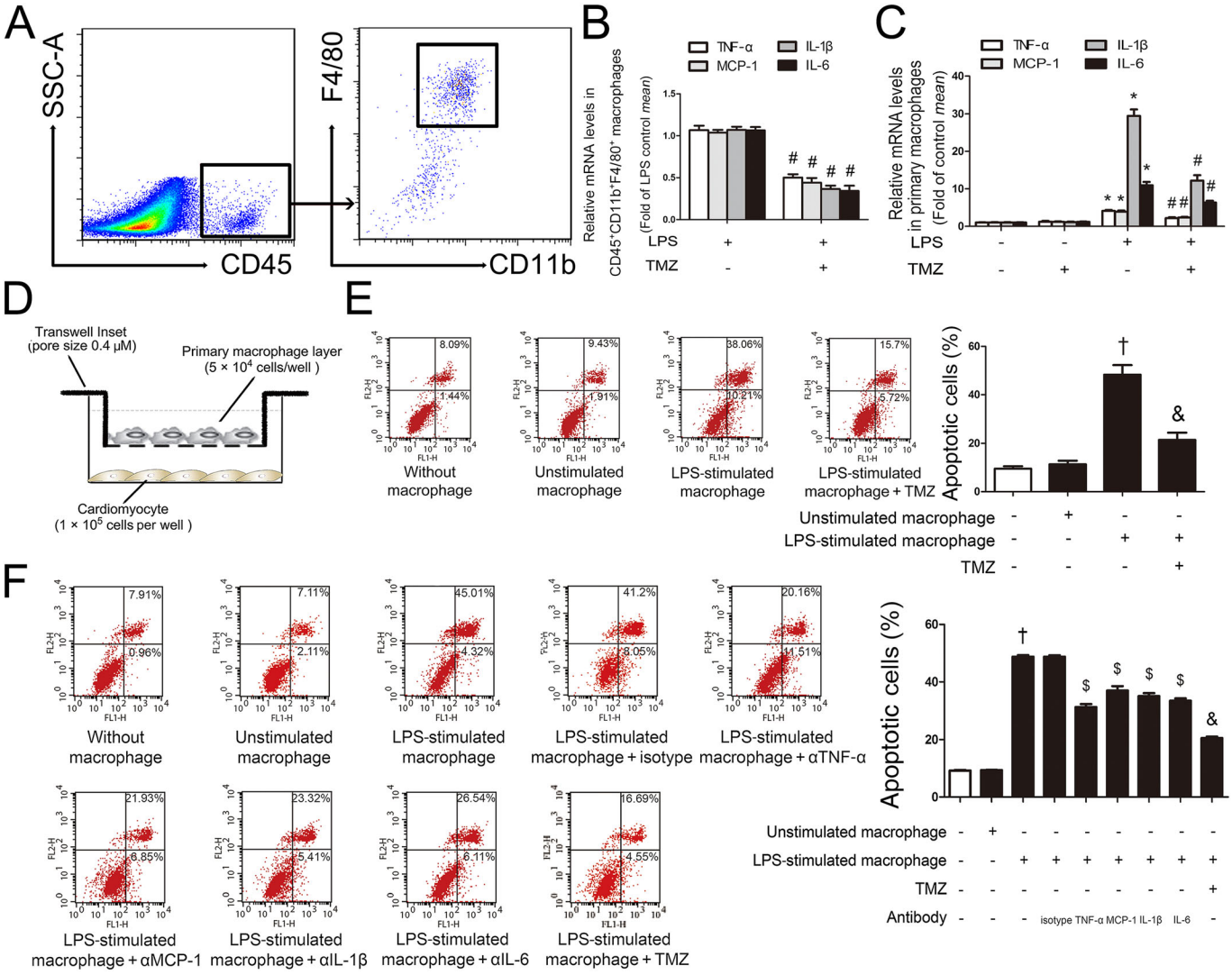

Figure 4

TMZ attenuated the cardiomyocyte apoptosis, mediated by the pro-inflammatory response of macrophages. (A) FACS gating strategy to identify $CD45^+CD11b^+F4/80^+$ cardiac macrophages. (B) TMZ-pretreated (20 mg · kg^{-1}, i.g., t.i.d., for 3 days) mice were subjected to LPS challenge (15 mg · kg^{-1}). $CD45^+CD11b^+F4/80^+$ cardiac macrophages were sorted from single cell suspensions prepared from the mice heart. The mRNA levels of pro-inflammatory cytokines of $CD45^+CD11b^+F4/80^+$ cardiac macrophages were examined by RT-PCR. (C) Peritoneal macrophages were pretreated with TMZ (20 μM) for 1 h and then stimulated with LPS (5 μg · mL^{-1}) for 6 h. RT-PCR was performed to measure levels of pro-inflammatory cytokines in peritoneal macrophages. (D) Peritoneal macrophages pretreated with TMZ (20 μM) were stimulated with LPS (5 μg · mL^{-1}) for 6 h and placed in transwell inserts above neonatal cardiomyocytes for 24 h. (E) Left, flow cytometry was performed to assay cardiomyocyte apoptosis; right, quantitative estimates of apoptotic cardiomyocytes in total cells. (F) Peritoneal macrophages pretreated with TMZ (20 μM) or antibodies to pro-inflammatory cytokines (20 μg · mL^{-1}) were stimulated with LPS for 6 h and placed in transwell inserts above neonatal cardiomyocytes for 24 h. Left, flow cytometry was performed to examine cardiomyocytes apoptosis; right, quantitative estimates of apoptotic cardiomyocytes in total cells. Data shown are means ± SEM of three separate experiments. $^*P < 0.05$ vs. control; $^{\#}P < 0.05$ vs. LPS-treated group; $^{\dagger}P < 0.05$ vs. unstimulated macrophage; $^{\&}P < 0.05$ vs. LPS-stimulated macrophage; $^{\$}P < 0.05$ vs. isotype antibody + LPS-stimulated macrophage. Data in (B) were analysed by Student's *t*-test. Other data were analysed by one-way ANOVA.

antibodies. TNF-α, CCL2, IL-1β and IL-6 were essential in the process of neonatal myocardial cells apoptosis when co-incubated with LPS-activated peritoneal macrophages (Figure 4). These results suggested that TMZ pretreatment reduced cardiomyocyte apoptosis mediated by the pro-inflammatory response of macrophages. Furthermore, TMZ also prevented LPS-induced cardiomyocyte apoptosis directly (Supporting Information Fig. S2a and b).

TMZ attenuated the ROS-mediated, pro-inflammatory response in macrophages, via Sirt1

We next investigated the molecular mechanisms of the anti-inflammatory effects of TMZ on peritoneal macrophages. Overproduction of ROS is thought to be harmful in sepsis; thus, we measured the antioxidant effects of TMZ in LPS-stimulated peritoneal macrophages. LPS-induced levels

of ROS were significantly reversed by TMZ, the effect of which was comparable with pretreatment with NAC, an effective ROS scavenger (Figure 5). At the same time, the pro-inflammatory cytokines were decreased when macrophages

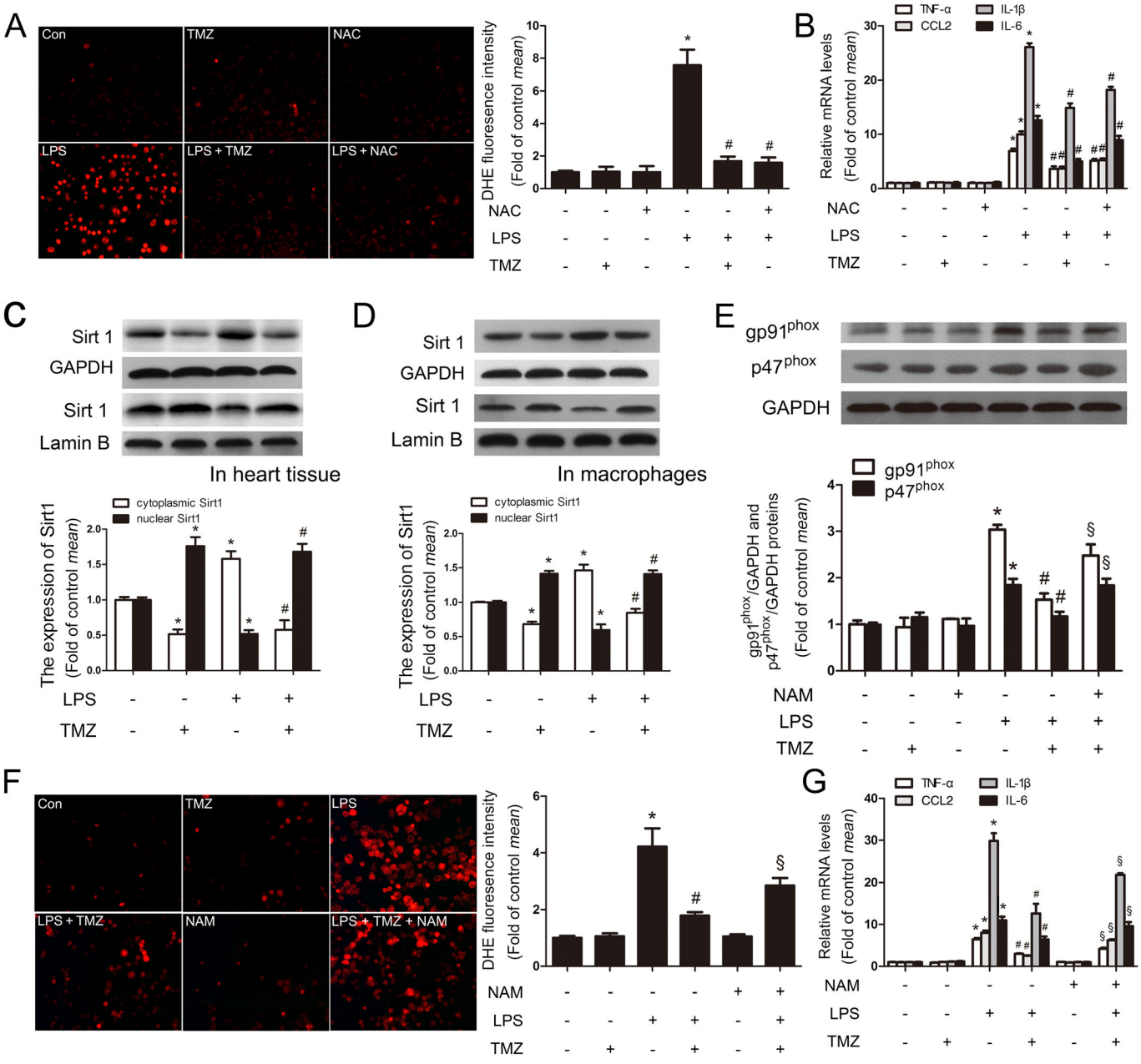

Figure 5

TMZ attenuated the ROS-mediated, pro-inflammatory response in macrophages, via Sirt1. Peritoneal macrophages were pretreated with TMZ (20 μM) or NAC (5 mM) for 1 h and then stimulated with LPS (5 μg · mL^{-1}) for 6 h. (A) ROS productions were detected by DHE staining. Left, representative images of the DHE staining in different groups; right, ROS productions were evaluated by quantification of mean fluorescence intensity in DHE staining. (B) RT-PCR showed the levels of pro-inflammatory cytokines. (C) Mice were pretreated with TMZ (20 mg · kg^{-1}, i.g., t.i.d.) for 3 days, and then injected with 15 mg · kg^{-1} LPS. The heart tissues were collected for examination of cytoplasmic and nuclear Sirt1 by Western blotting. (D) Peritoneal macrophages were pretreated with TMZ (20 μM) for 1 h and then stimulated with LPS (5 μg · mL^{-1}) for 6 h. Cytoplasmic and nuclear Sirt1 were examined by Western blotting. Values below the Western blots represent the densitometry analysis of cytoplasmic Sirt1/GAPDH and nuclear Sirt1/Lamin B. (E) Peritoneal macrophages were pretreated with or without TMZ (20 μM) or NAM (5 mM) for 1 h and then incubated with LPS (5 μg · mL^{-1}) for 6 h. Cell lysates were prepared and analysed for gp91^{phox} and p47^{phox} by Western blotting. Values below the Western blots represent the densitometry analysis of gp91^{phox}/GAPDH and p47^{phox}/GAPDH. (F) ROS production was detected by DHE staining. Left, representative images of the DHE staining in different groups; right, ROS production was evaluated by mean fluorescence intensity in DHE staining. (G) Additionally, the levels of pro-inflammatory cytokines were determined by RT-PCR. Data shown are means ± SEM of three independent experiments. *$P < 0.05$ vs. control; $^{\#}P < 0.05$ vs. LPS-treated group; $^{\S}P < 0.05$ vs. LPS + TMZ-treated group; one-way ANOVA.

were treated with TMZ or NAC after LPS challenge (Figure 5). These results indicated that TMZ attenuated LPS-induced inflammatory reactions via reduction of ROS.

Recent studies have reported that Sirt1 is involved in anti-oxidative and anti-inflammatory processes (Liu *et al.*, 2015; Trocme *et al.*, 2015). Our experiments showed that LPS up-regulated the expression of cytoplasmic Sirt1 in cardiac tissues from mice or in primary macrophages, and these effects were diminished by TMZ pretreatment. On the other hand, the effects on nuclear Sirt1 were the opposite. Taken together, TMZ treatment induced a translocation of Sirt1 from cytoplasm to nucleus, attenuating the effect of LPS (Figure 5). Moreover, TMZ clearly suppressed LPS-induced expression of the NADPH subunits gp91^{phox} and p47^{phox} (Figure 5). In addition, in the presence of a specific inhibitor of Sirt1 (NAM; Jackson *et al.*, 2003), the effects of TMZ were no longer decreased, indicating that Sirt1 signalling played an important role in the anti-oxidative effects of TMZ. The DHE staining analysis also showed that Sirt1 involved in the effect of TMZ on antioxidation (Figure 5) and, finally, decreased the mRNA expression of pro-inflammatory cytokines (Figure 5). In addition to the Sirt1-specific inhibitor NAM, these anti-oxidative and anti-inflammatory effects of TMZ were also blocked by Sirt1 siRNA (Supporting Information Fig. S3a–c). These results suggested that TMZ decreased the levels of ROS and then attenuated the inflammatory reactions via up-regulation of nuclear Sirt1 in peritoneal macrophages.

TMZ attenuated the macrophage pro-inflammatory responses through a Sirt1/AMPK/Nrf2/HO-1 signalling pathway

Previous studies have indicated that the important energy sensor AMPK was regulated by Sirt1 (Lan *et al.*, 2008). To further demonstrate whether AMPK was regulated by Sirt1 and the role of AMPK in the effects of TMZ on LPS-stimulated inflammatory reactions, the Sirt1 inhibitor NAM, Sirt1 siRNA and the AMPK inhibitor Compound C (Tian *et al.*, 2015) were applied in the following experiment.

As shown in Figure 6 and Supporting Information Fig. S3d, TMZ pretreatment significantly increased the phosphorylation of AMPK in LPS-induced peritoneal macrophages. However, pretreatment with NAM or Sirt1 siRNA blocked the effect of TMZ on AMPK phosphorylation, indicating AMPK was modulated by TMZ via Sirt1. As Nrf2 has been identified as the downstream partner of AMPK in inflammation, the protein level of Nrf2 and its target gene HO-1 were also examined in peritoneal macrophages. As expected, TMZ enhanced the expression of nuclear Nrf2 and HO-1 in LPS-stimulated peritoneal macrophages (Figure 6). However, in the presence of the AMPK inhibitor,

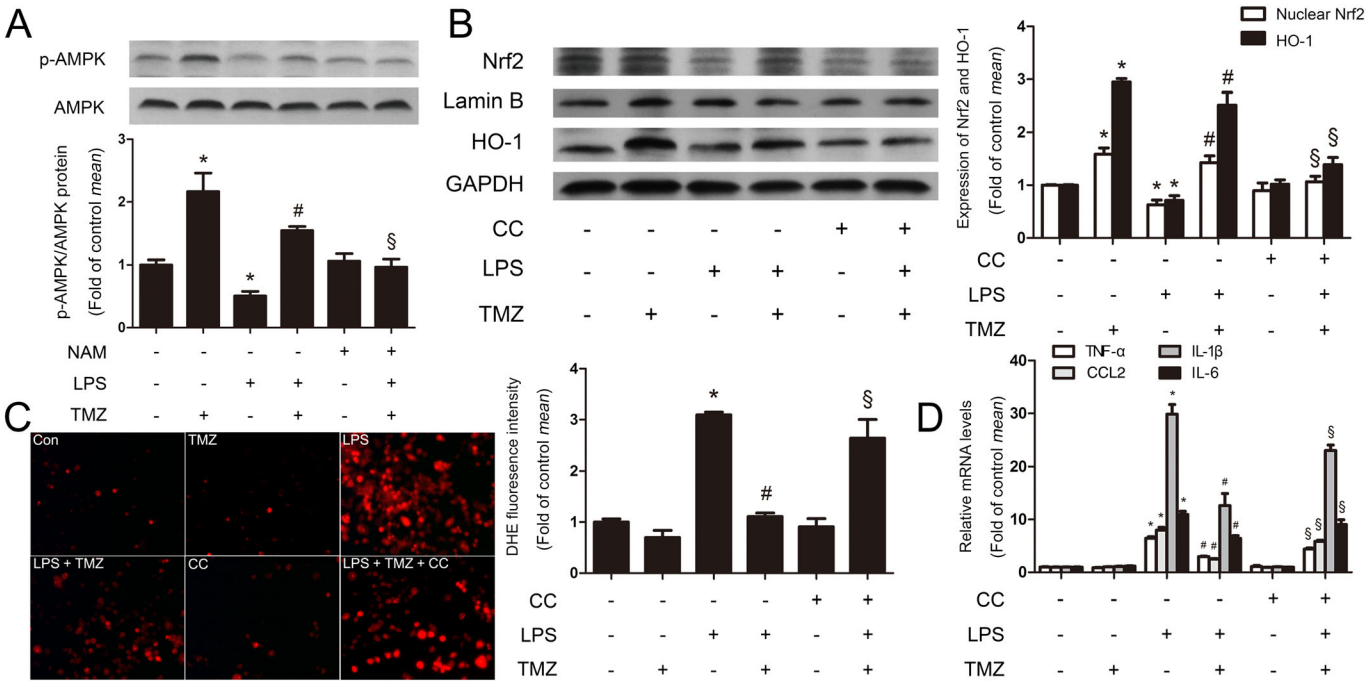

Figure 6

TMZ attenuated the macrophage pro-inflammatory responses through Sirt1/AMPK/Nrf2/HO-1 signalling. (A) Peritoneal macrophages were incubated with LPS (5 μg · mL^{-1}) in presence or absence of TMZ (20 μM) or the Sirt1-specific inhibitor NAM (5 mM), and cell lysates were prepared and analysed for AMPK and p-AMPK by Western blotting. Values below the Western blots represent the densitometry analysis of p-AMPK/AMPK. Peritoneal macrophages were pretreated with or without TMZ (20 μM) or Compound C (1 μM) for 1 h and then incubated with LPS (5 μg · mL^{-1}) for 6 h. (B) Nuclear Nrf2 and HO-1 were detected by Western blotting. (C) ROS production was assayed by DHE staining. Left, representative images of the DHE staining in different group; right, ROS production was evaluated by quantification of mean fluorescence intensity in DHE staining. (D) The levels of pro-inflammatory cytokines were measured by RT-RCR. Data were presented as mean ± SEM of three separate experiments. *$P < 0.05$ vs. control; $^{\#}P < 0.05$ vs. LPS; $^{\S}P < 0.05$ vs. LPS + TMZ-treated group; one-way ANOVA.

Compound C, the effects of TMZ on nuclear Nrf2 and HO-1 protein expression (Figure 6), ROS generation (Figure 6) and expression of mRNA for pro-inflammatory cytokines were ablated (Figure 6). Therefore, these results suggested that Sirt1/AMPK was involved in modulating ROS in inflammatory reactions via Nrf2 and HO-1 activation and, finally, attenuated the expression of pro-inflammatory cytokines.

TMZ attenuated the macrophage pro-inflammatory response through the Sirt1/PPARα signalling pathway

There is accumulating evidence that increased PPARα can attenuate inflammation (Smeets *et al.*, 2008). However, it is unclear whether TMZ activated PPARα by Sirt1 in LPS-induced inflammatory response in macrophages. As shown in Figure 7 and Supporting Information Fig. S3e, NAM or Sirt1 siRNA dramatically blocked the TMZ-induced increased levels of nuclear PPARα protein in LPS-stimulated peritoneal macrophages, suggesting that Sirt1 was essential for TMZ-induced PPARα activation. In addition, TMZ prevented LPS-induced increase in the content of p-IκBα and nuclear p65, and the effect was abolished by PPARα inhibitor GW6471 (Figure 7). These results revealed that TMZ inhibited the phosphorylation of IκBα and the influx of p65 to nuclei through Sirt1/PPARα. Consistent with the molecular changes, the levels of ROS were also reversed (Figure 7), indicating that TMZ could regulate ROS production by the Sirt1/PPARα pathway. Meanwhile, the inflammatory reactions were exacerbated in the presence of GW6471, even after pretreatment with TMZ after LPS stimulation (Figure 7). Hence, TMZ suppressed LPS-induced ROS generation through activation of the Sirt1/PPARα pathway, which was accompanied with p-IκBα/NF-κB inhibition and ultimately attenuated the pro-inflammatory response.

TMZ mitigated the cardiomyocyte apoptosis mediated by the pro-inflammatory response of macrophages, through the Sirt1/AMPK or Sirt1/PPARα pathway

Finally, to further determine whether TMZ attenuated LPS-induced neonatal cardiomyocyte apoptosis through the Sirt1/AMPK or the Sirt1/PPARα pathway, peritoneal macrophages were stimulated with LPS alone or LPS + TMZ or LPS + TMZ + inhibitors, and culture medium was added to cardiomyocytes (Figure 8). Results of flow cytometry showed that the culture medium from LPS-stimulated primary macrophages significantly increased apoptosis of cardiomyocytes,

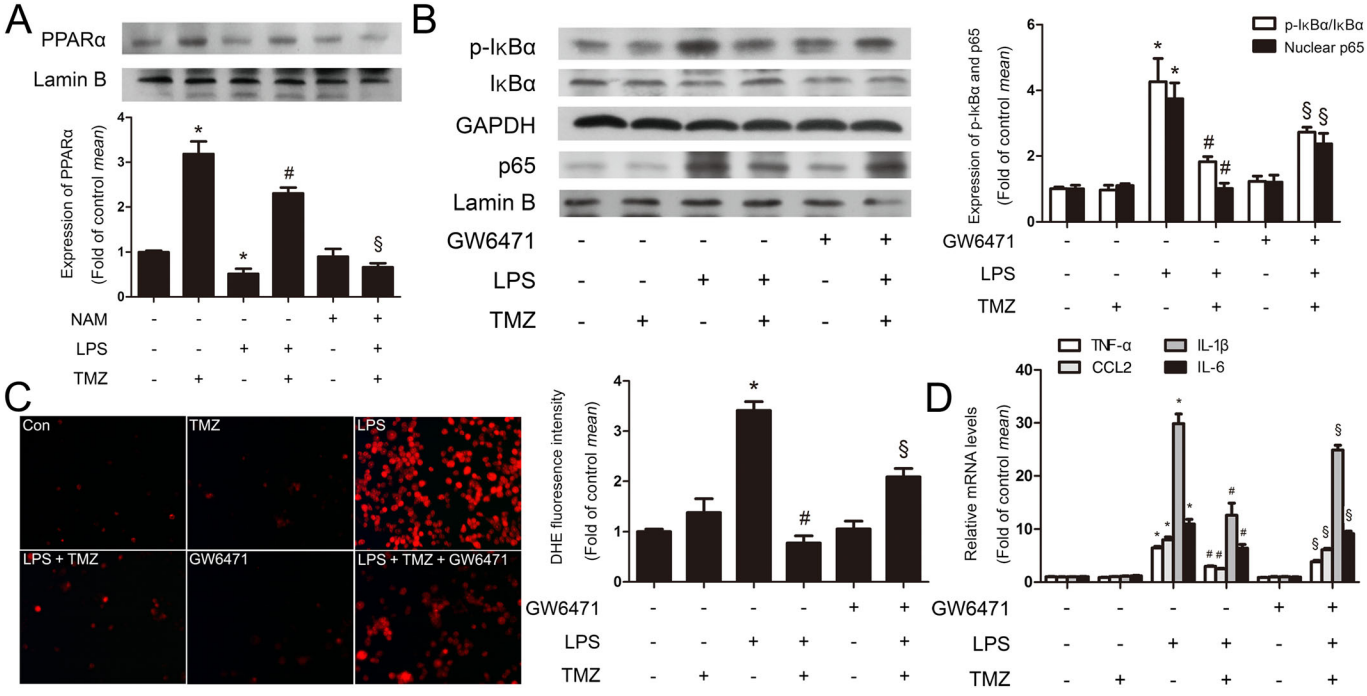

Figure 7

TMZ attenuated the macrophage pro-inflammatory response through Sirt1/PPARα signalling. (A) Peritoneal macrophages were incubated with LPS (5 μg · mL^{-1}) in presence or absence of TMZ (20 μM) or Sirt1-specific inhibitor NAM (5 mM). Representative Western blotting showed the expression of PPARα in nucleus. Values below the Western blots represent the densitometry analysis of PPARα/Lamin B. Peritoneal macrophages were pretreated with PPARα inhibitor GW6471 (3 μM) or TMZ (20 μM) for 1 h and then stimulated with LPS (5 μg · mL^{-1}) for 6 h. (B) The expression of p-IκBα and nuclear p65 were detected by Western blotting. (C) DHE staining showed the levels of ROS. Left, representative images of the DHE staining in different groups; right, ROS productions were evaluated by mean fluorescence intensity in DHE staining. (D) Pro-inflammatory cytokines were assessed by RT-PCR. Data were presented as mean ± SEM of three separate experiments. *$P < 0.05$ vs. control; $^{\#}P < 0.05$ vs. LPS; $^{\S}P < 0.05$ vs. LPS + TMZ-treated group; one-way ANOVA.

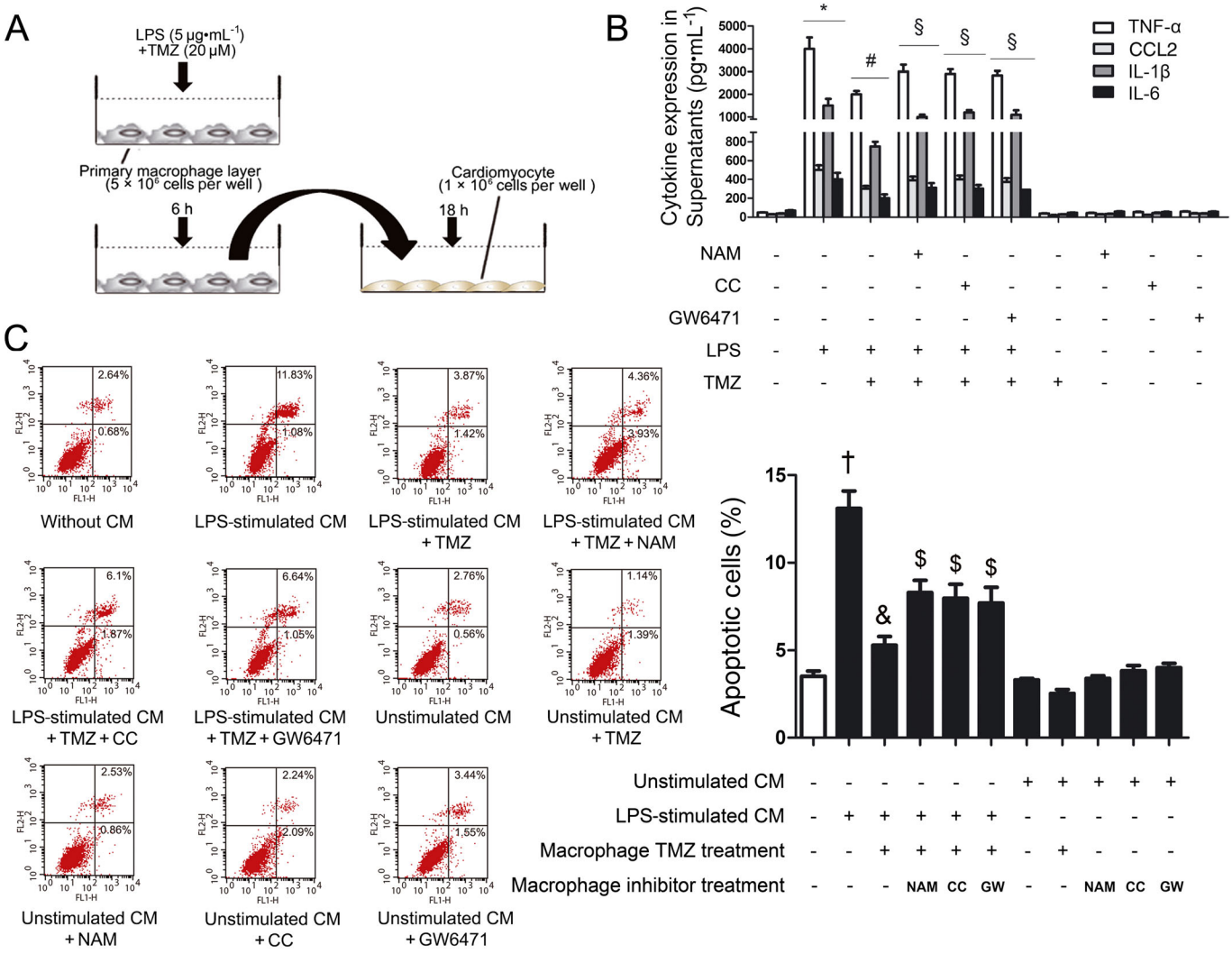

Figure 8

TMZ-mitigated macrophage pro-inflammatory response-mediated cardiomyocyte apoptosis through the Sirt1/AMPK or the Sirt1/PPARα pathway. (A) Peritoneal macrophages were stimulated with LPS alone or LPS + TMZ or LPS + TMZ + inhibitors, and the culture medium (CM) were added to cardiomyocytes. (B) Pro-inflammatory cytokine secretions in culture medium were determined by ELISA. (C) Left, flow cytometry was performed to examine cardiomyocyte apoptosis in the presence of NAM (5 mM) or Compound C (1 μM) or GW6471 (3 μM); right, quantitative estimates of apoptotic cardiomyocytes in total cells. Data shown are means ± SEM of three separate experiments. $^{*}P < 0.05$ vs. control; $^{\#}P < 0.05$ vs. LPS; $^{\S}P < 0.05$ vs. LPS + TMZ; $^{\dagger}P < 0.05$ vs. unstimulated CM; $^{\&}P < 0.05$ vs. LPS-stimulated CM; $^{\$}P < 0.05$ vs. LPS + TMZ-treated CM; one-way ANOVA.

whereas pretreatment with TMZ attenuated LPS-induced apoptosis. However, in the presence of NAM or CC or GW6471, the levels of inflammation were all increased (Figure 8) and the inhibitory effects of TMZ on LPS-induced apoptosis were all abolished (Figure 8). Therefore, TMZ decreased the cardiomyocyte apoptosis, which was induced by LPS-stimulated peritoneal macrophages through the Sirt1/AMPK or the Sirt1/PPARα pathway.

Discussion

Clinical evidence has shown that the 3-ketoacyl-CoA thiolase inhibitor, TMZ, exerts protective effects against ischaemia and reperfusion injury, leading to a reduction in the markers of myocardial damage, of oxidative stress, and thus, of inflammatory response (Bonello *et al.*, 2007; Di Napoli *et al.*, 2007; Martins *et al.*, 2011). But how TMZ regulates these effects is not completely understood, especially the inflammatory response. In our study, we demonstrated that TMZ ameliorated the pro-inflammatory response of macrophages, which induced cardiomyocyte apoptosis. This effect of TMZ was achieved by normalizing the Sirt1/AMPK/Nrf2/HO-1 and Sirt1/PPARα pathway in macrophages (Figure 9). Furthermore, although TMZ affected myocardial substrate consumption by shifting energy production from FFA to glucose oxidation (Kantor *et al.*, 2000; Onay-Besikci *et al.*, 2008), the genes involved in FFA metabolism (CD36, FABP3 and CPT-1) (Supporting Information Fig S4a–c) and

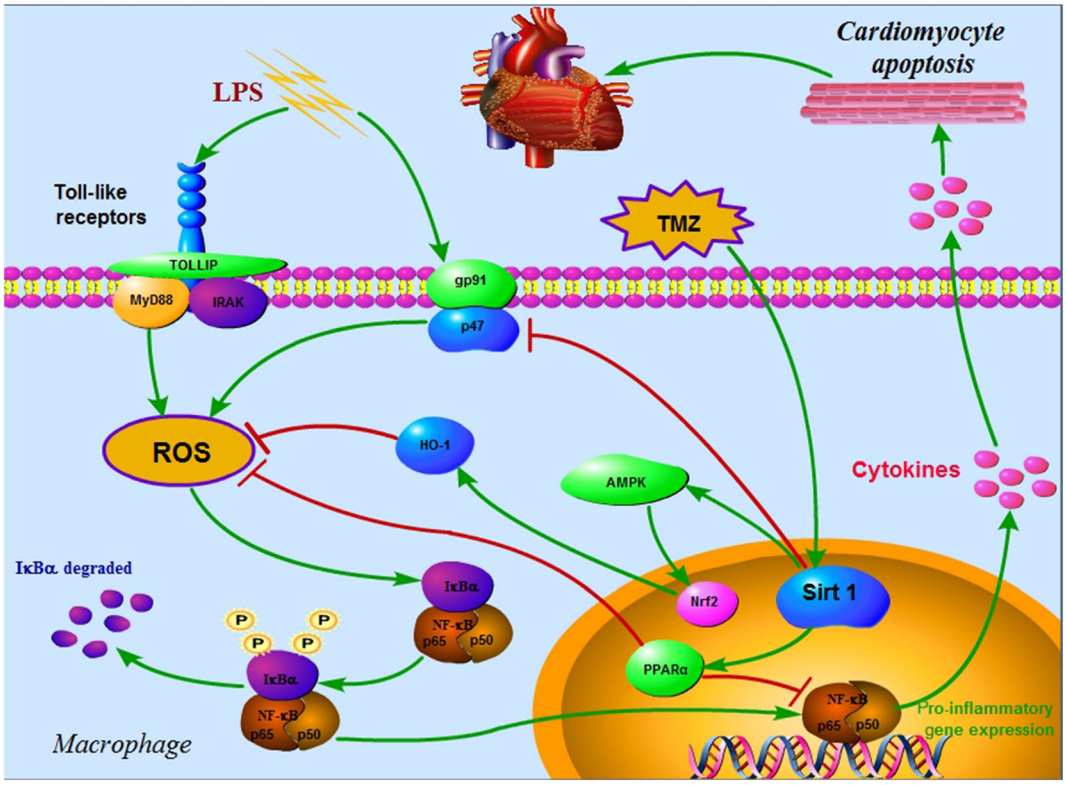

Figure 9

Schematic figure of possible signalling mechanisms of TMZ in LPS-induced, macrophage pro-inflammatory response-mediated, cardiomyocyte apoptosis. TMZ-ameliorated macrophage pro-inflammatory response, which induced cardiomyocytes apoptosis. This effect of TMZ was achieved by normalizing the Sirt1/AMPK/Nrf2/HO-1 and the Sirt1/PPARα pathways in macrophages. At the same time, the levels of ROS and pro-inflammatory cytokines were attenuated by activation of Sirt1, which played a central role against inflammation.

glucose metabolism [Glut4 and pyruvate dehydrogenase kinase isozyme 4 (PDK4)] (Supporting Information Fig. S4d and S4e) were not affected by TMZ in LPS-induced septic myocardial dysfunction. These findings may provide an innovative therapeutic strategy for myocardial dysfunction in sepsis.

In the excessive inflammatory response characteristic of of sepsis, macrophages synthesize and release pro-inflammatory cytokines, such as TNF-α, CCL2, IL-1β and IL-6, which are not only involved in the inflammatory response but also expand the inflammation, further developing the tissue injury and disease (Guzik *et al.*, 2003). It has been demonstrated that these inflammatory cytokines increased markedly after myocardial infarction and were involved in the subsequent myocardial injury (Nian *et al.*, 2004). Thus, we hypothesized that the excessive inflammatory response in macrophages during sepsis, was critically involved in the subsequent myocardial apoptosis. In our present study, levels of inflammatory markers, including TNF-α, CCL2, IL-1β and IL-6, were measured to evaluate the extent of systemic inflammation in a model of LPS-induced sepsis. To determine whether excessive inflammatory response in LPS-activated macrophages is involved in cardiomyocytes apoptosis, a macrophage–cardiomyocyte co-culture model was performed. Our findings suggested that TMZ significantly reduced LPS-induced macrophage pro-inflammatory response, accompanied with decreased levels of cardiomyocyte apoptosis. Furthermore, by adding antibodies of cytokines (TNF-α, CCL2, IL-1β and IL-6) in the co-culture model, we confirmed the deleterious role of cytokines produced by macrophages in causing cardiomyocyte apoptosis. Additionally, LPS induced myocardial infiltration by macrophages, while macrophages were not detected in TMZ pretreated mice. Bone marrow transplantation demonstrated that the improvement of cardiac function in TMZ > WT and TMZ > TMZ mice was associated with reduced infiltration of macrophages. Further, the reduced macrophage infiltration following TMZ was paralleled by decreased numbers of their precursors, $CD11b^{+}Ly6C^{+}$ monocytes, indicating that TMZ also affected the recruitment of monocytes.

Numerous studies have demonstrated the role of NADPH oxidase-dependent ROS generation in modulating TLR4 signalling, inflammatory response and disease pathogenesis (Fan *et al.*, 2003; Imai *et al.*, 2008). The NADPH oxidase complex is a major source of intracellular ROS generation in macrophages. The NADPH oxidase complex is composed of two transmembrane proteins: flavocytochrome b components ($gp91^{phox}$ and $p22^{phox}$) and four cytosolic proteins ($p47^{phox}$, $p67^{phox}$, $p40^{phox}$ and Rac) (Lambeth, 2004). Our findings suggested that TMZ decreased the expression of $gp91^{phox}$, $p47^{phox}$ and attenuated LPS-induced oxidative stress through

Sirt1, which activated downstream AMPK or PPARα, and finally attenuated inflammatory reactions.

The signal pathways involved in inflammatory response are grouped into pro-inflammatory pathways and anti-inflammatory pathways. The former includes NF-κB pathway, and the latter includes Nrf2 pathway. NF-κB pathway promotes the production of ROS and pro-inflammatory cytokines, particularly from immunocytes, such as macrophages (Hall *et al.*, 2005). In contrast, the Nrf2 pathway acts protectively against inflammation by activating antioxidant cascades (Guo and Ward, 2007). Our results revealed that Sirt1 induced by TMZ in macrophages on one hand coupled to AMPK to enhance the antioxidant Nrf2/HO-1 pathway and on the other hand coupled to PPARα to attenuate the expression of p-IκBα and nuclear p65, thus suppressing the NF-κB pathway.

To determine whether TMZ prevented cardiomyocyte apoptosis by decreasing the excessive inflammatory response in macrophages via the Sirt1/AMPK and Sirt1/PPARα pathway, culture medium from macrophages were added to cardiomyocytes and the macrophages were stimulated with LPS alone or LPS + TMZ or LPS + TMZ + inhibitors in advance. As expected, decreased inflammatory reactions in macrophages by TMZ through Sirt1/AMPK or Sirt1/PPARα pathway contributed to the rescue of apoptotic cardiomyocytes.

In conclusion, our results demonstrated that TMZ ameliorated LPS-induced myocardial dysfunction and cardiomyocyte apoptosis, effects that were dependent on attenuation of macrophage infiltration and pro-inflammatory responses. These effects of TMZ were achieved by normalizing the Sirt1/AMPK/Nrf2/HO-1 and the Sirt1/PPARα pathway in macrophages. At the same time, the levels of ROS were attenuated by TMZ by activation of Sirt1, which played a central role against inflammation. These findings may provide an innovative therapeutic strategy for myocardial dysfunction in sepsis.

Acknowledgements

This work was supported by grant from the National Natural Science Foundation of China (no. 31130031) and Changjiang Scholars and Innovative Research Team in University (no. IRT_14R20). The funders had no role in study design, data collection and analysis, decision to publish or preparation of the manuscript.

Author contributions

J. C. carried out the animal experiments and molecular studies, performed the statistical analysis and drafted the manuscript. J. L. carried out the bone marrow transplantation. L. Y. and G. R. participated in the animal experiments. S. C. and Q. N. helped drafting the manuscript. C. C. participated in the design of the study and the animal experiments and drafted the manuscript. D. W. W. conceived of the study and participated in its design and coordination and helped to draft the manuscript. All authors read and approved the final manuscript.

Conflict of interest

None to declare.

References

Alexander SPH, Benson HE, Faccenda E, Pawson AJ, Sharman JL, Spedding M *et al.* (2013a). The Concise Guide to PHARMACOLOGY 2013/14: Enzymes. Br J Pharmacol 170: 1797–1867.

Alexander SPH, Benson HE, Faccenda E, Pawson AJ, Sharman JL, Spedding M *et al.* (2013b). The Concise Guide to PHARMACOLOGY 2013/14: Nuclear Hormone Receptors. Br J Pharmacol 170: 1652–1675.

Bonello L, Sbragia P, Amabile N, Com O, Pierre SV, Levy S *et al.* (2007). Protective effect of an acute oral loading dose of trimetazidine on myocardial injury following percutaneous coronary intervention. Heart 93: 703–707.

Brown MA, Jones WK (2004). NF-kappaB action in sepsis: the innate immune system and the heart. Front Biosci 9: 1201–1217.

Curtis MJ, Bond RA, Spina D, Ahluwalia A, Alexander SP, Giembycz MA *et al.* (2015). Experimental design and analysis and their reporting: new guidance for publication in BJP. Br J Pharmacol 172: 3461–3471.

Daynes RA, Jones DC (2002). Emerging roles of PPARs in inflammation and immunity. Nat Rev Immunol 2: 748–759.

Di Napoli P, Di Giovanni P, Gaeta MA, Taccardi AA, Barsotti A (2007). Trimetazidine and reduction in mortality and hospitalization in patients with ischemic dilated cardiomyopathy: a *post hoc* analysis of the Villa Pini d'Abruzzo Trimetazidine Trial. J Cardiovasc Pharmacol 50: 585–589.

Dispersyn GD, Borgers M (2001). Apoptosis in the heart: about programmed cell death and survival. News Physiol Sci 16: 41–47.

Fan J, Frey RS, Malik AB (2003). TLR4 signaling induces TLR2 expression in endothelial cells via neutrophil NADPH oxidase. J Clin Invest 112: 1234–1243.

Fauvel H, Marchetti P, Chopin C, Formstecher P, Neviere R (2001). Differential effects of caspase inhibitors on endotoxin-induced myocardial dysfunction and heart apoptosis. Am J Physiol Heart Circ Physiol 280: H1608–H1614.

Guo RF, Ward PA (2007). Role of oxidants in lung injury during sepsis. Antioxid Redox Signal 9: 1991–2002.

Guzik TJ, Korbut R, Adamek-Guzik T (2003). Nitric oxide and superoxide in inflammation and immune regulation. J Physiol Pharmacol 54: 469–487.

Hall G, Singh IS, Hester L, Hasday JD, Rogers TB (2005). Inhibitor-kappaB kinase-beta regulates LPS-induced TNF-alpha production in cardiac myocytes through modulation of NF-kappaB p65 subunit phosphorylation. Am J Physiol Heart Circ Physiol 289: H2103–H2111.

Hu JP, Nishishita K, Sakai E, Yoshida H, Kato Y, Tsukuba T *et al.* (2008). Berberine inhibits RANKL-induced osteoclast formation and survival through suppressing the NF-kappaB and Akt pathways. Eur J Pharmacol 580: 70–79.

Imai Y, Kuba K, Neely GG, Yaghubian-Malhami R, Perkmann T, van Loo G *et al.* (2008). Identification of oxidative stress and Toll-like receptor 4 signaling as a key pathway of acute lung injury. Cell 133: 235–249.

Jackson MD, Schmidt MT, Oppenheimer NJ, Denu JM (2003). Mechanism of nicotinamide inhibition and transglycosidation by Sir2 histone/protein deacetylases. J Biol Chem 278: 50985–50998.

Kantor PF, Lucien A, Kozak R, Lopaschuk GD (2000). The antianginal drug trimetazidine shifts cardiac energy metabolism from fatty acid oxidation to glucose oxidation by inhibiting mitochondrial long-chain 3-ketoacyl coenzyme A thiolase. Circ Res 86: 580–588.

Kitada M, Kume S, Imaizumi N, Koya D (2011). Resveratrol improves oxidative stress and protects against diabetic nephropathy through normalization of Mn-SOD dysfunction in AMPK/SIRT1-independent pathway. Diabetes 60: 634–643.

Lambeth JD (2004). NOX enzymes and the biology of reactive oxygen. Nat Rev Immunol 4: 181–189.

Lan F, Cacicedo JM, Ruderman N, Ido Y (2008). SIRT1 modulation of the acetylation status, cytosolic localization, and activity of LKB1. Possible role in AMP-activated protein kinase activation. J Biol Chem 283: 27628–27635.

Liu TF, Vachharajani V, Millet P, Bharadwaj MS, Molina AJ, McCall CE (2015). Sequential actions of SIRT1-RELB-SIRT3 coordinate nuclear-mitochondrial communication during immunometabolic adaptation to acute inflammation and sepsis. J Biol Chem 290: 396–408.

Martins GF, Siqueira Filho AG, Santos JB, Assuncao CR, Bottino F, Carvalho KG *et al.* (2011). Trimetazidine on ischemic injury and reperfusion in coronary artery bypass grafting. Arq Bras Cardiol 97: 209–216.

McDonald TE, Grinman MN, Carthy CM, Walley KR (2000). Endotoxin infusion in rats induces apoptotic and survival pathways in hearts. Am J Physiol Heart Circ Physiol 279: H2053–H2061.

McGrath JC, Lilley E (2015). Implementing guidelines on reporting research using animals (ARRIVE etc.): new requirements for publication in BJP. Br J Pharmacol 172: 3189–3193.

McGrath JC, McLachlan EM, Zeller R (2015). Transparency in Research involving Animals: The Basel Declaration and new principles for reporting research in BJP manuscripts. Br J Pharmacol 172: 2427–2432.

Michan S, Sinclair D (2007). Sirtuins in mammals: insights into their biological function. Biochem J 404: 1–13.

Minhas KM, Khan SA, Raju SV, Phan AC, Gonzalez DR, Skaf MW *et al.* (2005). Leptin repletion restores depressed β-adrenergic contractility in ob/ob mice independently of cardiac hypertrophy. J Physiol 565: 463–474.

Mo C, Wang L, Zhang J, Numazawa S, Tang H, Tang X *et al.* (2014). The crosstalk between Nrf2 and AMPK signal pathways is important for the anti-inflammatory effect of berberine in LPS-stimulated macrophages and endotoxin-shocked mice. Antioxid Redox Signal 20: 574–588.

Nian M, Lee P, Khaper N, Liu P (2004). Inflammatory cytokines and postmyocardial infarction remodeling. Circ Res 94: 1543–1553.

Onay-Besikci A, Ozkan SA (2008). Trimetazidine revisited: a comprehensive review of the pharmacological effects and analytical techniques for the determination of trimetazidine. Cardiovasc Ther 26: 147–165.

Opal SM, Scannon PJ, Vincent JL, White M, Carroll SF, Palardy JE *et al.* (1999). Relationship between plasma levels of lipopolysaccharide (LPS) and LPS-binding protein in patients with severe sepsis and septic shock. J Infect Dis 180: 1584–1589.

Pawson AJ, Sharman JL, Benson HE, Faccenda E, Alexander SP, Buneman OP *et al.* (2014). The IUPHAR/BPS Guide to PHARMACOLOGY: an expert-driven knowledge base of drug targets and their ligands. Nucleic Acids Res 42 (Database Issue): D1098–D1106.

Planavila A, Iglesias R, Giralt M, Villarroya F (2011). Sirt1 acts in association with PPARalpha to protect the heart from hypertrophy, metabolic dysregulation, and inflammation. Cardiovasc Res 90: 276–284.

Smeets PJ, Teunissen BE, Planavila A, de Vogel-van den Bosch H, Willemsen PH, van der Vusse GJ *et al.* (2008). Inflammatory pathways are activated during cardiomyocyte hypertrophy and attenuated by peroxisome proliferator-activated receptors PPARalpha and PPARdelta. J Biol Chem 283: 29109–29118.

Tian W, Li W, Chen Y, Yan Z, Huang X, Zhuang H *et al.* (2015). Phosphorylation of ULK1 by AMPK regulates translocation of ULK1 to mitochondria and mitophagy. FEBS Lett 589: 1847–1854.

Trocme C, Deffert C, Cachat J, Donati Y, Tissot C, Papacatzis S *et al.* (2015). Macrophage-specific NOX2 contributes to the development of lung emphysema through modulation of SIRT1/MMP-9 pathways. J Pathol 235: 65–78.

Turdi S, Han X, Huff AF, Roe ND, Hu N, Gao F *et al.* (2012). Cardiac-specific overexpression of catalase attenuates lipopolysaccharide-induced myocardial contractile dysfunction: role of autophagy. Free Radic Biol Med 53: 1327–1338.

Vivot K, Langlois A, Bietiger W, Dal S, Seyfritz E, Pinget M *et al.* (2014). Pro-inflammatory and pro-oxidant status of pancreatic islet in vitro is controlled by TLR-4 and HO-1 pathways. PLoS One 9: e107656.

Ward PA (2009). The sepsis seesaw: seeking a heart salve. Nat Med 15: 497–498.

Zhang L, Freedman NJ, Brian L, Peppel K (2004). Graft-extrinsic cells predominate in vein graft arterialization. Arterioscler Thromb Vasc Biol 24: 470–476.

Zhou X, Li C, Xu W, Chen J (2012). Trimetazidine protects against smoking-induced left ventricular remodeling via attenuating oxidative stress, apoptosis, and inflammation. PloS one 7: e40424.

Supporting Information

Additional Supporting Information may be found in the online version of this article at the publisher's web-site:

http://dx.doi.org/10.1111/bph.13386

Figure S1 Cardiac function in mice receiving bone marrow transplants was associated with the numbers of F4/80$^+$ macrophages in heart tissues. Scatter plot of cardiac function parameters (y-axis) and the numbers of F4/80$^+$ macrophages (x-axis) determined by immunohistochemical staining in heart tissues. (A) Correlation between LVEF values and the number of F4/80$^+$ macrophages. (B) Correlation between LVFS values and the number of F4/80$^+$ macrophages. (C) Correlation between dp/dt max values and the number of F4/80$^+$ macrophages. (D) Correlation between dp/dt min values and the number of F4/80$^+$ macrophages. Pearson's correlation coefficient was used to measure the linear relationship between numbers of F4/80$^+$ macrophages and LVEF values, LVFS values, dp/dt max values and dp/dt min value.

Figure S2 TMZ attenuated cardiomyocyte apoptosis induced by LPS. Neonatal cardiomyocytes were pretreated with TMZ (20 μM) for 1 hour and then stimulated with LPS (5 $\mu g \cdot ml^{-1}$) for 6 hours. (A) Apoptosis of cardiomyocytes was analyzed with flow cytometry, using annexin Vand propidium iodide (PI). (B) The apoptosis of different groups and P values. Data

were presented as mean ± SEM of three separate experiments and were analyzed by one-way ANOVA using SPSS software.

Figure S3 TMZ attenuated ROS-mediated macrophage pro-inflammatory responses via Sirt1. Peritoneal macrophages were first transfected with si-Sirt1 or random siRNA using lipo 2000 for 24 hours. After transfection, cells were pretreated with TMZ (20 μM) for 1 h and then stimulated with LPS (5 $\mu g \cdot ml^{-1}$) for 6 h. (A) The ROS levels in macrophages were measured by DHE staining. (B) ROS productions were evaluated by quantification of mean fluorescence intensity in DHE staining. (C) RT-PCR revealed the expression of pro-inflammatory cytokines. Cell lysates were prepared and analyzed for phosphorylated (p)-AMPK (D) and nuclear PPARα (E) expression by Western blotting. Values below the Western blots represent the densitometry analysis of p-AMPK/AMPK and nuclear PPARα/Lamin B. Data were presented as mean ± SEM of three separate experiments and were analyzed by one-way ANOVA analysis using SPSS software. *$P < 0.05$ vs. control; $^{\#}$ $P < 0.05$ vs. LPS; § $P < 0.05$ vs. LPS + TMZ treated group; † $P < 0.05$ vs. Lipo 2000 control.

Figure S4 TMZ did not affect the shift from fatty acids to glucose metabolism in LPS-stimulated heart. C57BL/6 mice were pretreated with TMZ (20 $mg \cdot kg^{-1}$, i.g., t.i.d.) or saline three times a day for 3 days, followed by i.p injection of LPS (15 $mg \cdot kg^{-1}$) (n=8 in each group). The mice were sacrificed 6 hours after LPS stimulation and the heart tissue were collected to prepare RNA samples. (A–F) RT-PCR analysis showed the relative mRNA levels of CPT-1, CD36, FABP3, GLUT4 and PDK4. All values were normalized internally to 18S RNA expression and to the normal control sets. Data were presented as mean ± SEM of three independent experiments. Data were analyzed by one-way ANOVA analysis using SPSS software.